UNIVERSIDADE FEDERAL DO RIO GRANDE DO SUL

Seminário do Programa de Pós-Graduação em Engenharia Química

IX Oktoberfórum – PPGEQ

19, 20 e 21 de outubro de 2010

# DETERMINATION OF FLOW-INDUCED STRESSES IN CAVITY FILLING

**João A. P. de Oliveira[1], Andréia R. Machado[1], Jovani L. Favero[2], Argimiro R. Secchi[3], Nilo S.M. Cardozo[4*], Hrvoje Jasak[5]**

[1] LASIM - Departamento de Engenharia Química, UFRGS – IFSul – japo@sapucaia.ifsul.edu.br,
[2] Laboratório de Termofluidodinâmica (LTFD) – PEQ/COPPE – UFRJ/CT –
[3] COPPE- Programa de Engenharia Química, - UFRJ/CT –
[4*] LASIM/LATEP - Departamento de Engenharia Química, UFRGS – nilo@enq.ufrgs.br –
R. Eng. Luis Englert, s/n. Campus Central. CEP: 90040-04 Porto Alegre, RS
[5] FSB/Wikki – Faculty of Mechanical Engineering and Naval Architecture, University of Zagreb, Croatia - h.jasak@wikki.co.uk

***Abstract:*** *Thin wall injection molding process has significant differences in relation to conventional injection molding process. Two important factors that affect residual flow-induced stresses in injected plastic parts were studied: cavity thickness and injection velocity. A numerical approach based on the solver viscoelasticInterFoam, to solve the viscoelastic flow problem of cavity filling in injection molding, was introduced. The implemented methodology was used in the calculation of isothermal flow-induced stresses during the filling stage of a simple 2D geometry (planar parallel plates geometry) with different cavity thicknesses and flow velocities. The viscoelastic stress results showed that flow-induced stresses increase significantly and cannot be neglected in the analysis of thin wall injection molding. The correspondent non-isothermal flow is also being studied and some results obtained with a decoupled method are presented.*

***Keywords:*** *thin wall, polymer injection molding, flow-induced stresses, viscoelastic flow, PTT model, OpenFOAM*

## 1. Introduction

Injection molding is one of the most important processes of the polymer industry. This process can be separated in three stages: filling, packing, and cooling. Its numerical simulation is very important both for mold project and operating conditions.

An important issue in the simulation of injection molding is the prediction of residual stresses as a function of the processing parameters (CAO et al., 2008; WANG & YANG, 2005). The residual stresses in plastic parts can be classified in flow-induced (entropic) and thermally- and pressure-induced (elastic energy) residual stresses (DOUVEN et al., 1995; ZOETELIEF et al., 1996).

BAAIJENS (1991) calculated the stresses developed in conventional injection process (parts with thickness higher than 1 mm), and observed that the thermally-induced stresses are one order of magnitude higher than the flow-induced stresses. Based on this result, a great number of papers published since then, on residual stresses in plastic parts, have neglected the flow-induced stresses (WANG & YANG, 2005; DOUVEN et al., 1995; ZOETELIEF et al., 1996).

However, this type of residual stresses is always present at some level in injected molded parts and may, in some critical cases, play an important role in their final properties. The presence of flow-induced residual stresses in polymeric parts is due to the fact that their complete relaxation is partially avoided by the very high cooling rates used in the process (DOUVEN et al., 1995). The potential influence of residual stresses on the final properties of the parts is related to the effect of frozen molecular orientation on the anisotropy of the mechanical, thermal and optical properties, and on the long term dimensional stability of the parts.

In this sense it is worthy to consider the production of thin wall parts. Thin wall process can be defined as the process where cavities have thicknesses lower than 1 mm and a flow length-to-thickness ratio larger than 100 (CHEN et al., 2007). The importance of thin wall parts has been increasing in the last years due to advantages as higher production rate and reduction in part size and raw material consumption. In comparison to conventional injection processes, the reduction in thickness leads to higher cooling rates and requires higher pressure and injection velocity, with the consequent increase of shear stress during filling stage. So, the relative importance of flow-induced stresses is expected to be even more pronounced in thin wall parts than in conventional processes. In spite of this, the approach of neglecting flow-induced stresses has also been applied to calculate the residual stresses in thin wall parts (WANG & YANG, 2005), although there were not found in the literature data which prove that this extension of the results for

conventional injection is indeed valid for thin wall parts production.

In this context, the goal of the present work is to evaluate the importance of flow-induced stresses in thin wall processes, through the numerical analysis of the isothermal filling stage of a simple thin wall geometry (rectangular flat plate) with a simplified Phan–Thien–Tanner (PTT) fluid. This analysis was performed using a methodology which is being developed in this work and whose basic validation has been presented in OLIVEIRA et al. (2010). Non-isothermal processes are being studied and some preliminary results will be presented at the end of the paper.

## 2. Methodology

### *2.1 Governing Equations*

Under isothermal conditions, the governing equations for the flow in the filling step of the injection molding are mass and momentum conservation equations. Since in the filling step, the melt flow can be considered incompressible, the mass balance can be written as:

$$\underline{\nabla} \cdot \underline{u} = 0 \qquad (1)$$

where $\underline{u}$ is the velocity vector.

The equation of conservation of momentum can be written as:

$$\frac{\partial \rho \underline{u}}{\partial t} + \underline{\nabla} \cdot \left(\rho \underline{u}\underline{u}\right) - \underline{\nabla} \cdot \underline{\underline{\tau}} = -\underline{\nabla} p + \rho \underline{g} \qquad (2)$$

where ρ is the density, $t$ is the time, $\underline{\underline{\tau}}$ is the shear stress tensor, $p$ is the pressure, and $\underline{g}$ is the gravity acceleration.

To complete the mathematical description of this flow problem a constitutive model for the stress tensor is required. In this work, three different constitutive models were used:

- Newtonian fluid (NF):

$$\underline{\underline{\tau}} = 2\mu \underline{\underline{D}} \qquad (3)$$

where μ is the Newtonian viscosity and $\underline{\underline{D}}$ is strain rate tensor, given by:

$$\underline{\underline{D}} = 1/2\left(\underline{\nabla u} + \underline{\nabla u}^T\right) \qquad (4)$$

- generalized Newtonian fluids (GNF):

$$\underline{\underline{\tau}} = 2\eta\left(\dot{\gamma}\right)\underline{\underline{D}} \qquad (5)$$

where $\eta\left(\dot{\gamma}\right)$ is the viscosity function and $\dot{\gamma}$ is the shear rate.

- and the simplified Phan–Thien–Tanner (SPTT) model (CAO et al., 2008; COELHO et al., 2002):

$$\left[1 + \frac{\varepsilon\lambda}{\eta} tr\left(\underline{\underline{\tau}}\right)\right]\underline{\underline{\tau}} + \lambda \overset{\nabla}{\underline{\underline{\tau}}} = 2\eta \underline{\underline{D}} \qquad (6)$$

where λ is the relaxation time, ε is a dimensionless parameter, $\overset{\nabla}{\underline{\underline{\tau}}}$ is the upper-convected derivative:

$$\overset{\nabla}{\underline{\underline{\tau}}} = \frac{D\underline{\underline{\tau}}}{Dt} - \underline{\underline{\tau}} \cdot \underline{\nabla u} - \left(\underline{\nabla u}\right)^T \cdot \underline{\underline{\tau}} \qquad (7)$$

and $D\underline{\underline{\tau}}/Dt$ is the material derivative:

$$\frac{D\underline{\underline{\tau}}}{Dt} = \frac{\partial \underline{\underline{\tau}}}{\partial t} + \underline{u} \cdot \underline{\nabla}\underline{\underline{\tau}} \qquad (8)$$

Under non-isothermal conditions, the equation of conservation of energy is necessary and, in terms of temperature, can be written as (KENNEDY, 1995):

$$\rho C_p \left(\frac{\partial T}{\partial t} + \underline{u} \cdot \nabla T\right) = \kappa \underline{\nabla}^2 T + \underline{\underline{\pi}} : \left(\underline{\nabla u}\right) \qquad (9)$$

where $C_p$ is the specific heat, $T$ is the temperature, $\kappa$ is the thermal conductivity and $\underline{\underline{\pi}}$ is the total stress tensor.

In the analysis of non-isothermal flows, the temperature dependence of the parameters of the rheological model has also to be considered. In this work, as discussed in the next section, only the generalized Newtonian model was used in non-isothermal calculations. In this case, the viscosity was evaluated by the Cross-WLF model (CAO et al., 2008):

$$\eta\left(\dot{\gamma}\right) = \frac{\eta_0\left(T, p\right)}{1 + \left(\eta_0 \dot{\gamma}/\tau^*\right)^{1-n}} \qquad (10)$$

where $\tau^*$ is is the shear stress level of the asymptotic transition region between the power law and Newtonian fluids, and $\eta_0(T, p)$ is the zero shear rate viscosity, with the temperature dependence of $\eta_0(T, p)$ being described by the Williams, Landel and Ferry (WLF):

$$\eta_0\left(T, p\right) = D_1 \exp\left\{-\frac{A_1\left[T - T^*\left(p\right)\right]}{\tilde{A}_2 + D_3 p + \left[T - T^*\left(p\right)\right]}\right\} \qquad (11)$$

where $T^*\left(p\right) = D_2 + D_3 p$ and $A_1$, $\tilde{A}_2$, $D_1$, $D_2$ and $D_3$ are parameters which depend on the material.

### *2.2 Numerical implementation*

The governing equations were discretized by the finite volume method (FVM), formulated with collocated grid, in OpenFOAM (OpenFOAM version 1.5, 2009), using the solver viscoelasticInterFoam (FAVERO et al., 2009). This solver uses the VOF (Volume of Fluid) method to capture the interface. In this method, a phase transport equation is solved to determine the relative volume fraction of the two phases in each computational cell:

$$\frac{\partial f}{\partial t} + \nabla \cdot \left(f \underline{u}\right) = 0 \qquad (12)$$

where $f$ is the phase fraction, with $f = 0$ corresponding to a cell totally filled by air, while $f = 1$ corresponds to a cell

totally filled by polymer. Values of *f* between 0 and 1 correspond to a cell of the interface polymer/air.

In the solver viscoelasticInterFoam, velocity/pressure and stress calculations are decoupled. At each time step, the PISO algorithm (JASAK, 1996) is used to obtain pressure and velocity fields from the continuity and momentum equations using stress values calculated in the previous iteration and, subsequently, the constitutive equation is solved to update the stress field. To achieve convergence for each time step a SIMPLE correction loop is used into the PISO loop (FAVERO et al., 2009).

Another aspect to consider is the numerical approach for the analysis of non-isothermal flows, which can be done by coupled or decoupled methods (DOUVEN et al., 1995). In the decoupled method, the velocity, pressure and temperature fields are solved using a GNF model to provide the flow kinematics and, subsequently, the induced stress are calculated explicitly from the viscoelastic model. In the coupled method, the viscoelastic behavior of the polymer melt is considered in the calculation of the flow kinematics. Although earlier studies suggest that flow induced stresses calculated by the two methods compare satisfactorily (DOUVEN et al.; 1995), the recent developments in the analysis of viscoelastic flows provide higher accuracy in the analysis and make it worthy to develop a more definitive conclusion in this sense. That is why both methods are being implemented in this work. However, results will be shown only for the decoupled method whose implementation is already finished.

The discretization scheme for gradients was Gaussian integration with linear interpolation (central differencing) of values from cell centers to face. For the advective terms of the momentum and VOF equations the Gauss discretization scheme was used. The interpolation scheme for the dependent fields was the limited linear differencing for velocity, and limited van Leer or upwind for the phase fraction. For stress divergent it was used the Gauss integration with upwind and linear schemes. For discretization of the diffusive term the Gauss scheme was used, and the linear interpolation scheme was used for the Laplacian. The explicit non-orthogonal correction scheme was used for the surface normal gradient (JASAK, 1996). An interface compression scheme developed for OpenFOAM is used to get a sharp interface (HEMIDA, 2010). For the advective member of the energy equation it was used the Gauss integration with upwind scheme.

For the solution of resultant linear algebraic equations, the following iterative methods were used: conjugated gradient (PCG) with diagonal incomplete-Cholesky preconditioner for pressure and bi-conjugated gradient (PBiCG) with diagonal incomplete-LU preconditioner for stress, temperature and velocity (JASAK, 1996).

### *2.3 Initial and boundary conditions*

As initial condition an internal field equal to zero was defined for all variables: $\underline{u}=0$, $p=0$, $f=0$, $\underline{\underline{\tau}}=0$.

During cavity filling it was assumed a constant velocity at the inlet, no slip at the walls and zero velocity gradient at the outlet.

It was assumed zero pressure gradient at the inlet and at the walls, and fixed value zero for pressure at the outlet. For volume fraction, *f was* set equal to 1 at the inlet, and zero gradient was specified at the walls and at the outlet. For the shear stress tensor, a fixed value equal to zero was used for stress at the inlet, and zero gradient at walls and at outlet. For non-isothermal processes uniform temperature of 504 K (in order to reduce thermal loss at front flow) was set as initial internal temperature field, while temperatures of 504 and 333 K, respectively, were specified at the inlet and at the wall.

### *2.4 Studied Geometries*

The geometries used in the tests performed in this work were planar parallel plates, with lengths between 20 and 60 mm and thicknesses from 0.4 to 2 mm, in order to cover the range from thin wall to conventional mold dimensions.These geometries, together with the meshes used, are represented in Figure 2.1. All meshes were hexahedral and were generated with the blockMesh utility of the OpenFOAM. Fine and homogeneous meshes, with low aspect ratio, were used in order to achieve a good compression of the interface of the front of the flow. In the non-isothermal cases the mesh used was refined at the walls.

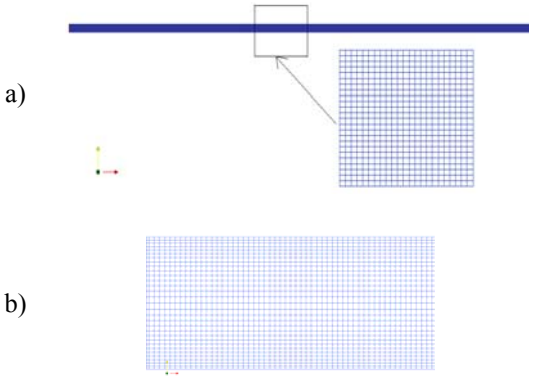


Figure 2.1 Geometry and mesh used in analysis of flow-induced stresses:
a) isothermal; b) non-isothermal.

### *2.5 Equipment*

A four processors computer with intel® core™2 quad cpu q6600 @ 2,40 ghz with operational system linux, kernel linux 2.6.24, ubuntu 8.04 was used in all simulations.

## 3. Results and Discussion

### *3.1 Viscoelastic solver evaluation in the Newtonian limit*

Previously to the its application in the comparison of the residual stresses in conventional and thin wall molding, a study on the consistency of the stress predictions with the solver viscoelasticInterFoam was accomplished. This study consisted in checking the

predictions of the solver for the simplified Phan-Thien-Tanner model in the Newtonian limit (i.e, attributing null values for the parameters λ and ε of Eq. 6) through the comparison against those of the solver interFoam. The value of η used for both simulations was $4.673 \times 10^3$ Pas. A plate with 1 mm of thickness and 20 mm of length and a homogeneous mesh with 13,500 elements were used in this test.

The predicted profiles of the *x*-component of the velocity ($u_x$) along the central line of the channel for an inlet velocity of $1 ms^{-1}$, in the filling time of 0.2 seconds, are presented in Figure 3.1, while Figure 3.2 shows the $u_x$ profiles in the thickness direction at $x = 2.5$ mm. The stress profiles ($\tau_{xy}$) at $x = 2.5$ mm are presented in Figure 3.3. The good agreement observed between the predictions of the two solvers shows that the solver viscoelasticInterFoam describes adequately the Newtonian limit.

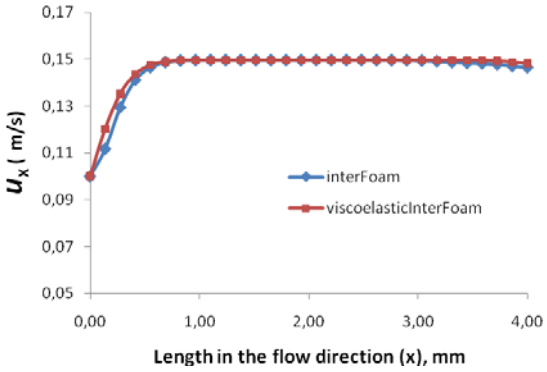


**Figure 3.1** $u_x$ profiles in the flow direction with solvers interFoam and viscoelasticInterFoam for constant inlet velocity of 0,1 $ms^{-1}$and filling time of 0.2 s.

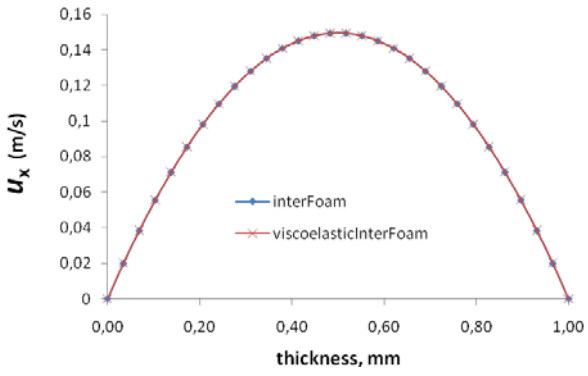


**Figure 3.2** $u_x$ profiles in the thickness direction at x = 2.5 mm with solvers interFoam and viscoelasticInterFoam.

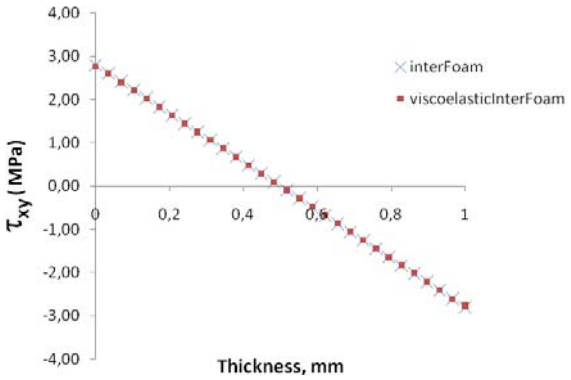


**Figure 3.3** Stress profiles in the thickness direction, at x = 2.5 mm, with solvers interFoam and viscoelasticInterFoam in the Newtonian limit.

*3.2 Comparison of flow-induced stresses in conventional and thin wall parts under isothermal conditions*

In this section, the flow of a viscoelastic fluid described by the simplified Phan-Thien-Tanner model (SPTT) in planar parallel plates geometry is studied and the results for different thickness and velocities are presented. The values of the SPTT model parameters used in this work were: λ = 0.1652, η = 1.321 x $10^4$ Pa s, and ε = 0.3, which are representative of a polystyrene sample at 448K (ROOZENDAAL, 1994).

Figure 3.4 presents the profile of first normal stress difference after 0.64 s of filling for a thickness of 2 mm and an inlet velocity of 0.09 $m.s^{-1}$, which are parameters representative of a conventional injection mold process. These results are of the same order of magnitude of those reported in the literature for first normal stress difference generated with other methodologies for similar geometry and flow parameters (CAO et al., 2008; DOUVEN et al., 1995; ZOETELIEF et al., 1996), although a quantitative comparison is not possible due to intrinsic differences in flow geometry and thermal effects.

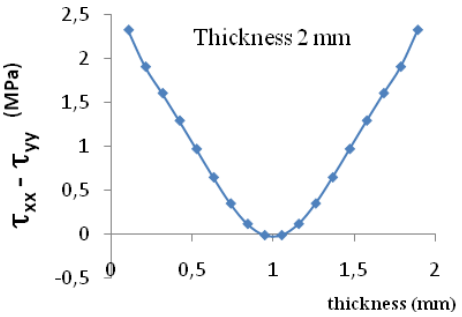


**Figure 3.4** Profile of first normal stress difference along the thickness for a plate with thickness of 2 mm at $x = 0{,}03$ m (inlet velocity: 0.09 m/s).

Figure 3.5 presents the profiles of the first normal stress difference after 0.05 s of filling at an inlet velocity of 3.5 $m.s^{-1}$ for three different thicknesses corresponding

to typical conditions used in the production of thin wall parts. As could be expected, the lower the cavity thickness the higher the stress levels found, which is due to the increase of the shear rate with the decrease of the thickness for a fixed velocity. However, the most relevant aspect in these results is the fact that, in all cases, the values of first normal stress were at least one order of magnitude higher than those corresponding to conventional injection molding conditions (Figure 3.4).

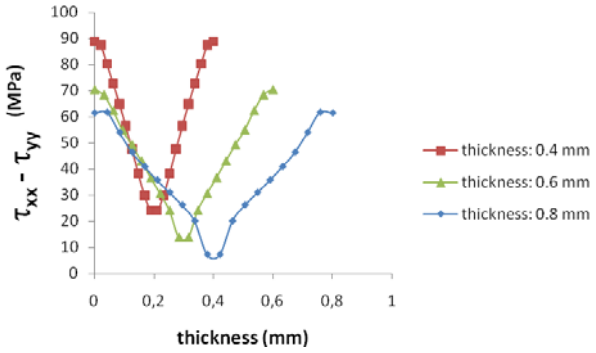


**Figure 3.5** Profiles of the first normal stress difference along the thickness at $x$ = 0.03 m and $t$ = 0.05 s for plates with thicknesses of 0.4, 0.6 and 0.8 mm.

Similar results were found when varying the inlet velocity in a typical range of the injection of thin wall parts for a thickness of 1 mm (Figure 3.6).

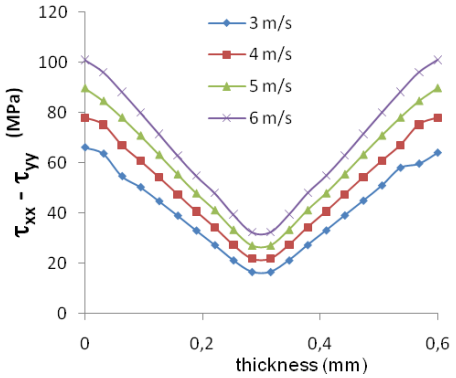


**Figure 3.6** Profiles along the thickness of the first normal stress difference in x = 0,03 m (thickness: 1 mm).

Besides the significant increase in the magnitude of the flow induced stresses described above for thin wall processing conditions, it must be considered that the magnitude of thermally-induced stresses is expected to decrease for lower part thicknesses (because of the higher uniformity in the polymer mass cooling). So, the presented results indicate that flow-induced stresses cannot be neglected in the analysis of thin wall injection molding.

*3.3 Preliminary results for non-isothermal conditions*

In the preliminary tests using the decoupled method for non-isothermal flow, a geometry with 20 mm of length and 1 mm of thickness was used. The thermal properties and the Cross-WLF model constants are given in Table 1. The SPTT parameters were the same used for isothermal processes.

**Table 1.** Thermal parameters for Polystyrol 165 H (BASF)

| Parameters | Units | Values |
|---|---|---|
| $Cp$ | J/kgC | 1975 |
| $k$ | W/mK | 0.155 |
| $n$ | - | 0.2202 |
| $\tau^*$ | Pa | 3.6027E+04 |
| $D_1$ | Pas | 2.1110E+12 |
| $D_2$ | K | 373.15 |
| $D_3$ | - | 0 |
| $A_1$ | - | 28.313 |
| $A_2$ | K | 51.6 |

Figure 3.7 shows the results obtained with the isothermal solver and with the non-isothermal decoupled method for the profiles of the first normal stress difference after 0.2 s of filling for an inlet velocity of 0.1 m.s$^{-1}$. In the non-isothermal solution, the first normal stress difference presents a maximum shifted to the center of the thickness of the plate, which is not present in the isothermal solution. This is due to the fact that the isothermal solution does not take into account the increase of viscosity near the cooled cavity walls which causes narrowing of the effective flow area. This effect can be observed in Figures 3.8 and 3.9 where the profiles of $u_x$ and shear rate, respectively, are presented.

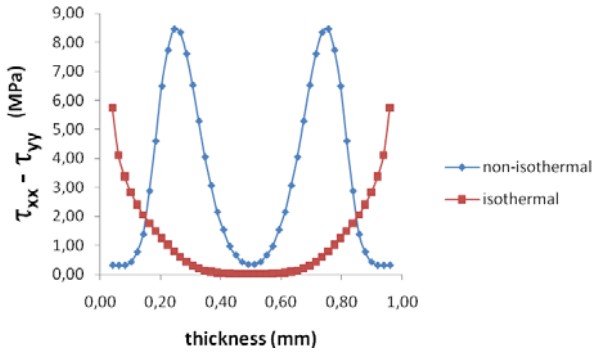


**Figure 3.7** Profiles along the thickness of the first normal stress difference in a plate with thickness of 1 mm, calculated for an isothermal and a non-isothermal process, at x=0.01 m for the time t = 0.2s.

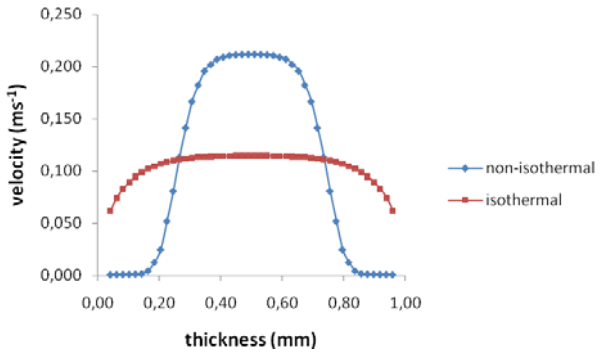


**Figure 3.8** Profiles along the thickness of the x-directed velocity in a plate with thickness of 1 mm, calculated for an isothermal and a non-isothermal process, for the time t = 0.2s.

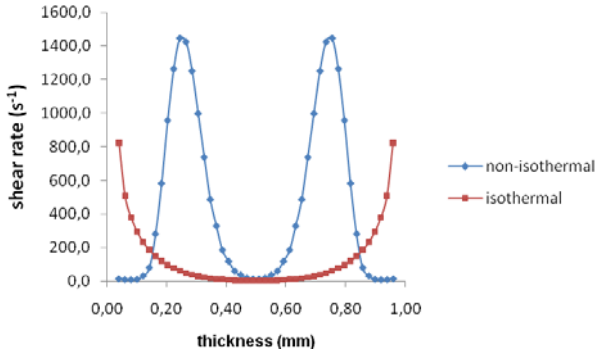


**Figure 3.9** Profiles along the thickness of the shear rate in a plate with thickness of 1 mm, calculated for an isothermal and a non-isothermal process, for the time t = 0.2s.

Results for three points, at different distances from the gate (inlet), are presented in Figure 3.10. As expected, the stress level decays as the point considered is farther from the gate.

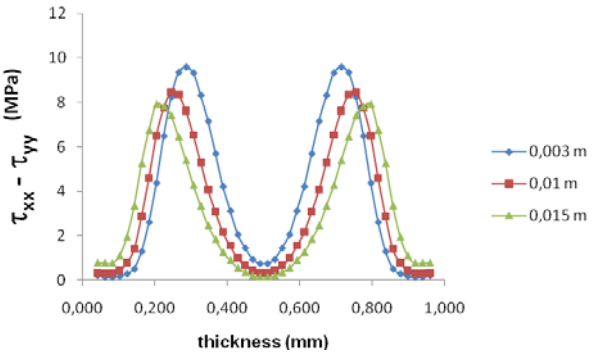


**Figure 3.10** Profiles along the thickness of the first normal stress difference in a plate with thickness of 1 mm, calculated for three different distances of the gate with non-isothermal solver for the time t = 0.2s.

All these non-isothermal profiles of the first normal stress difference (Figures 3.7 and 3.10) are qualitatively in agreement with those reported in the literature for similar flow conditions (CAO et al., 2008; DOUVEN et al., 1995), both in shape and order of magnitude.

## 4. Conclusions

This paper presented a methodology based in the solver viscoleasticinterfoam for the analysis of mold filling in injection molding processes. The application of the implemented methodology in the analysis of flow induced stresses of a viscoelastic fluid described by the simplified Phan-Thien-Tanner model indicated that these stresses cannot be neglected in the production of thin wall injection molding. The study of non-isothermal processes with a decoupled method has presented results in qualitatively agreement with literature. The next step of the work is determination of flow-induced stresses with a non-isothermal coupled method where viscoelastic behaviour is considered in the determination of the kinematics of the problem.

## *Acknowledgements*

*João A. P. de Oliveira is very grateful to the Instituto Federal Sul-Rio-Grandense for the support to do this work.*

## 5. References

BAAIJENS, F.P.T. Calculation of Residual Stresses in injection molded products. *Rheologica Acta*, v. 30, p. 284 – 299, 1991.

CAO, W.; SHEN, C.; ZHANG, C.; WANG, L. Computing flow-induced stresses of injection molding based on the Phan-Thien-Tanner model. *Archive of Applied Mechanics*, v. 78, p. 363 – 377, 2008.

CHEN, C.-S.; CHEN, T.-J.; CHIEN, R. –D.; CHEN, S.-C. Investigation on the weldline strength of thin-wall injection molded ABS parts. *International Communications in Heat and Mass Transfer*, vol. 34, p. 448 – 455, 2007.

COELHO, P.M.; PINHO,. F.T.; OLIVEIRA, P.J. Fully developed forced convection of the Phan – Thien – Tanner fluid in ducts with a constant wall temperature. *Internacional Journal of Heat and Mass Transfer*, v. 45, p. 1413 – 1423, 2002.

DOUVEN, L.F.A., BAAIJENS, F.P.T. and MEIJER, H.E.H. The computation of properties of injection – moulded products. *Progress in Polymer Science*, v. 20, p. 403 – 457, 1995.

FAVERO, J.L.; CARDOZO, N. S. M.; SECCHI, A. R.; JASAK, H. Simulação do inchamento de extrudado e do experimento rod-climbing usando o software openfoam. Anais do 10º CONGRESSO BRASILEIRO DE POLÍMEROS, 2009, Foz do Iguaçu, Proceedings.

HEMIDA, H.; OpenFOAM tutorial: Free surface tutorial using interFoam and rasInterFoam. Chalmers University of Technology, SE-412 96 Göteborg, Sweden.

http://www.tfd.chalmers.se/~hani/kurser/OS_CFD_2007/HassanHemida/Hassan_Hemida_VOF.pdf (10/01/2010).

JASAK, H. *Error analysis and estimation for the finite volume method with applications to fluid flows*. Doctorate Thesis, Imperial College of Science, Technology & Medicine, University of London, Londres, Inglaterra, 1996.

KENNEDY, P. *Flow analysis of injection molds*. Hanser Publishers, Munique, 1995.

OpenFOAM version 1.5. (2009) available in http://www.openfoam.com

OLIVEIRA, J.A.P.; MACHADO, A.R.; FAVERO, J.L.; SECCHI, A. R.; CARDOZO, N. S. M.; JASAK, H. Numerical analysis of flow-induced stress in isothermal flow of amorphous polymer in thin wall cavity filling. In: XII INTERNATIONAL MACROMOLECULAR COLLOQUIUM, 2010, Gramado, Proceedings.

ROOZENDAAL, R.A.J.G. *Transient viscoelastic flow around a cylinder*. Master's Thesis, Eindhoven University of Technology, Eindhoven, Holanda, 1994.

WANG, T.; YOUNG, W. Study on residual stresses of thin-walled injection molding. *European Polymer Journal*, v. 41, p. 2511 – 2517, 2005.

ZOETELIEF, W.F.; DOUVEN, L.F.A.; INGEN-HOUSZ, A.J. Residual thermal stresses in injection molded products. *Polymer Engineering and Science*, v. 36, p. 1886 – 1896, 1996.